Influence of TiO$_2$ Film Thickness on the Electrochemical Behaviour of Dye-Sensitized Solar Cells

V. Baglio[*], *M. Girolamo, V. Antonucci, A. S. Aricò*

CNR-ITAE Institute, via Salita S. Lucia sopra Contesse, 5 - 98126 Messina, Italy
[*]E-mail: baglio@itae.cnr.it

A commercial TiO$_2$ powder was deposited on F-doped SnO$_2$ (FTO) glass substrates by a spray coating technique with different thicknesses (6, 10 and 14 μm) to be used as photo-anode in dye-sensitized solar cells (DSSCs). N3 dye was adsorbed on each TiO$_2$ film for 16 h. The resulting electrodes were used to form dye-sensitized solar cells in combination with conventional electrolyte and counter-electrode. The cells were investigated by I-V characteristics and electrochemical impedance spectra. The cell formed with a TiO$_2$ film of 10 μm thickness reached the best performance. This thickness resulted as the best compromise in terms of absorption of incident light on the N3 dye, reduction of the recombination processes and suitable series and charge transfer resistance

1. INTRODUCTION

Dye-sensitized solar cells (DSSCs) are potentially low-cost photovoltaic devices alternative to p-n junctions [1-5]; they consist of a sensitizing dye, a nanoporous metal oxide film, an electrolyte and a counter electrode [6-10]. Light is absorbed by the sensitizer, which is anchored to the surface of a wide band gap semiconductor. The use of sensitizers having a broad absorption band in conjunction with oxide films of nanocrystalline morphology permits to harvest a large fraction of sunlight [11-13]. Usually the working electrode in these systems is a TiO$_2$ nanocrystalline film comprising of a three-dimensional network of interconnected 15–20 nm-sized nanoparticles sintered onto a conductive glass substrate [14]. As opposed to silicon-based devices where the semiconductor absorbs the light and transports the released charge carriers, the two tasks are separated in a DSSC system [6]. On illumination, the surface-adsorbed panchromatic dye absorbs photons giving rise to a jump of electrons from HOMO to LUMO which lies above the conduction band of the semiconductor. The dye in the excited state injects electrons into the conduction band of the semiconductor resulting in charge

separation. The oxidized dye is quickly reduced to its ground state by the iodide/tri-iodide redox species in the electrolyte before it can recapture the injected electron. Meanwhile, the injected electron is transported in the conduction band of the semiconductor by diffusion [15] to the charge-collecting conductive glass substrate from where it performs useful work in an external circuit. Through this circuit, electrons return to the cell at the counter electrode to reduce the redox species in the electrolyte.

Suitable photoconversion efficiencies [15] have been reported with these systems. The best efficiencies have been measured on a very low geometrical area (about 0.25 cm^2) and by using a multilayer approach which consists in expensive and time consuming procedures [16-20]. Usually, an optimized electrode is formed by using various procedures and treatments to give high electrochemical performance. FTO, after cleaning, is usually immersed in 40 mmol L^{-1} TiCl$_4$ aqueous solution at 70°C for 30 min and successively washed with water and ethanol. The glass is then treated at 450°C for 30 minutes [16]. Afterwards, a TiO$_2$ paste is coated on this modified FTO glass by doctor blade or screen printing techniques to obtain a TiO$_2$ film of 8-15 μm. This film is dried at 125°C. Successively, a TiO$_2$ light-scattering layer of 4-5 μm is added by using titania particles of about 200 nm in size. The double-layer TiO$_2$ film is gradually heated under an airflow up to 500°C [16]. According to this procedure, the preparation of an optimized electrode is quite expensive and time consuming for a large scale production. Moreover, the use of pre- and post-layers to improve adhesion and favour light-scatter properties, respectively, makes more complicate the understanding of the absorption layer properties that usually play the main role in the electrochemical cells. In this work, our approach was consisting of a very simple procedure to deposit the TiO$_2$ layer on the F-doped SnO$_2$ (FTO) glass substrates by a spray technique and successive heat treatment at 450°C, without any further process. The effect of TiO$_2$ layer thickness on the photo-electrochemical performance was investigated and the different results were interpreted on the basis of electrochemical diagnostics. A geometrical area of 1 cm^2 was used in our investigation.

2. EXPERIMENTAL

Photo-anodes and counter-electrodes were prepared on FTO glass (sheet resistance: 15Ω/□) substrates [21]. The TiO$_2$ paste for the photo-anode was prepared from commercial powder (Degussa P25) and deposited by a spray technique onto the substrate [21]. Afterwards, electrodes were sintered at 450°C for 30 minutes; the sintering process allowed the titanium dioxide nanocrystals to sinter and join together, in order to ensure electrical contact and mechanical adhesion on the glass. Dye sensitization was carried out by immersing the sintered electrodes in 0.2 mM N3 solution (Solaronix) in ethanol for about 16 hours. Electrolyte consisted of 0.4M LiI, 0.04M I$_2$, 0.3M 4-tertbutylpyridine (TBP) and 0.4M tetrabutylammonium iodide (TBAI) in Acetonitrile [22]. The Platinum counter electrode was prepared by depositing the hexachloro platinic acid based solution on FTO glass substrate, followed by sintering at 450°C for 30 minutes.

Current-voltage curves of the devices were recorded under simulated AM 1.5 solar illumination (Osram, 300W) at 25°C. The incident light intensity was adjusted to 100 mW cm^{-2} by using a

photometer (3M Photodine Inc.). The cells operating under simulated solar illumination were connected to an Autolab Potentiostat/Galvanostat (Metrohm) equipped with a Frequency Response Analyzer (FRA). The active area of the cells was 1 cm^2. Electrochemical Impedance Spectroscopy (EIS) measurements were carried out at room temperature in the frequency range 1 MHz-0.1 Hz at open circuit voltage (OCV); the amplitude of potential pulse was 0.01 V.

Scanning Electron Microscopy (SEM) analysis of TiO$_2$-coated FTO glasses was carried out by a FEI XL30 SFEG microscope. UV/vis spectra were carried out on a Hewlett-Packard model 8453 spectrometer.

3. RESULTS AND DISCUSSION
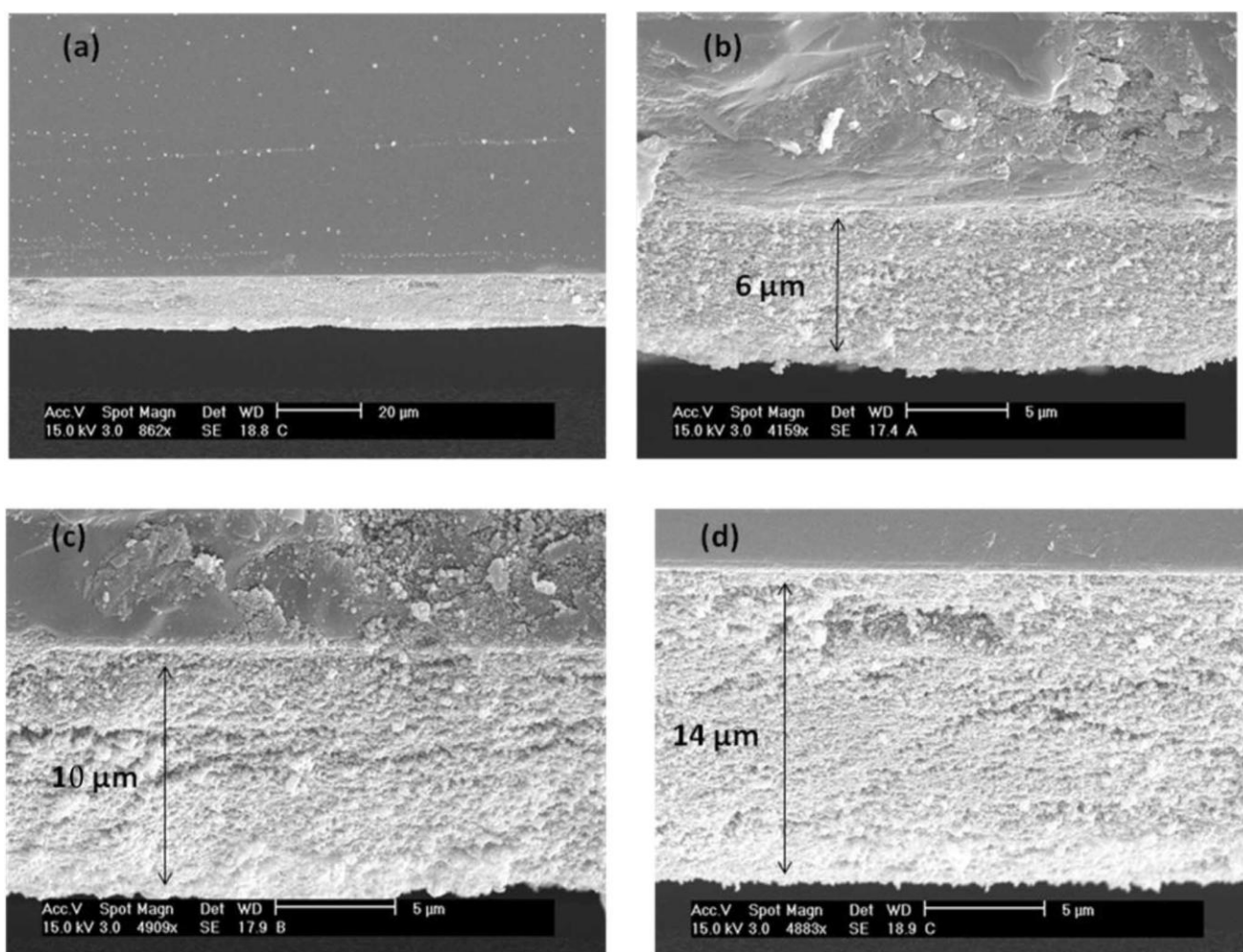
Figure 1. SEM cross-sectional images of TiO$_2$-coated FTO glasses at low magnification (a) and at high magnification (b), (c) and (d) with the estimation of TiO$_2$ thickness.

Fig. 1 shows cross-sectional SEM images of the TiO$_2$-coated FTO glasses after the sintering process at 450°C. The grains appear well connected each other with suitable mesoporosity to allow for

a formation of an extended electrode-electrolyte interface. The different TiO_2 thicknesses (6, 10 and 14 μm) onto the FTO glass are clearly observed in Fig. 1 b, c and d.
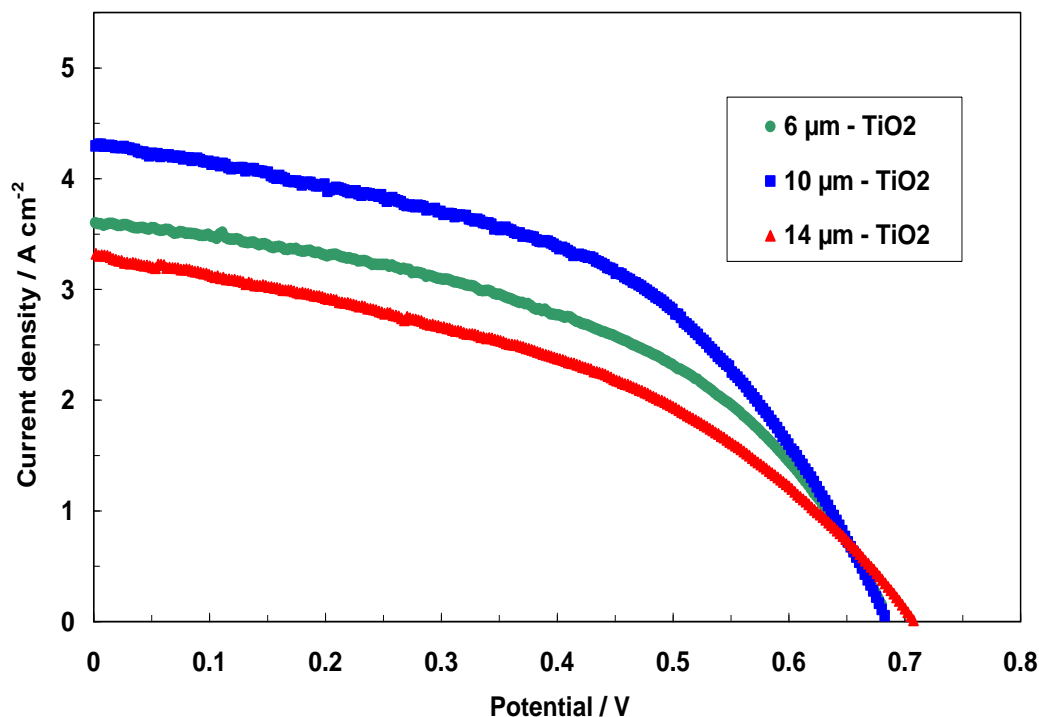
Figure 2. j–V curves for DSSCs using TiO_2 at different thicknesses as photo-anodes.

Fig. 2 shows the photocurrent-voltage characteristics for the DSSCs based on TiO_2 films with different thicknesses.

The conversion efficiency was calculated as follows:

$$\eta(\%) = \frac{V_{OC} \, j_{SC} FF}{P_S}$$

where P_S stands for the power density of the incident illumination, and the fill factor is calculated by:

$$FF = \frac{V_{mm} j_{mm}}{V_{OC} j_{SC}}$$

where j_m and V_m are respectively current density and voltage for maximum power output.

The conversion efficiencies (η), fill factors (FF), short circuit current densities (j_{SC}) and open-circuit photo-voltages (V_{OC}) for the different DSSCs using various TiO_2 thicknesses at the photo-anode are summarized in Table 1.

Table 1. Performance characteristics for the different DSSCs using various TiO$_2$ thicknesses at the photo-anode.

TiO$_2$ thickness (µm)	Voc (V)	Jsc (mA cm^{-2})	FF	η (%)
6	0.68	3.6	0.5	1.2
10	0.69	4.3	0.5	1.44
14	0.71	3.3	0.42	1.0

The photo-electrode with a thickness of 10 µm showed the best performance in terms of conversion efficiency, short circuit current density and fill factor; the open-circuit photo-voltage was the largest for the electrode of 14 µm.
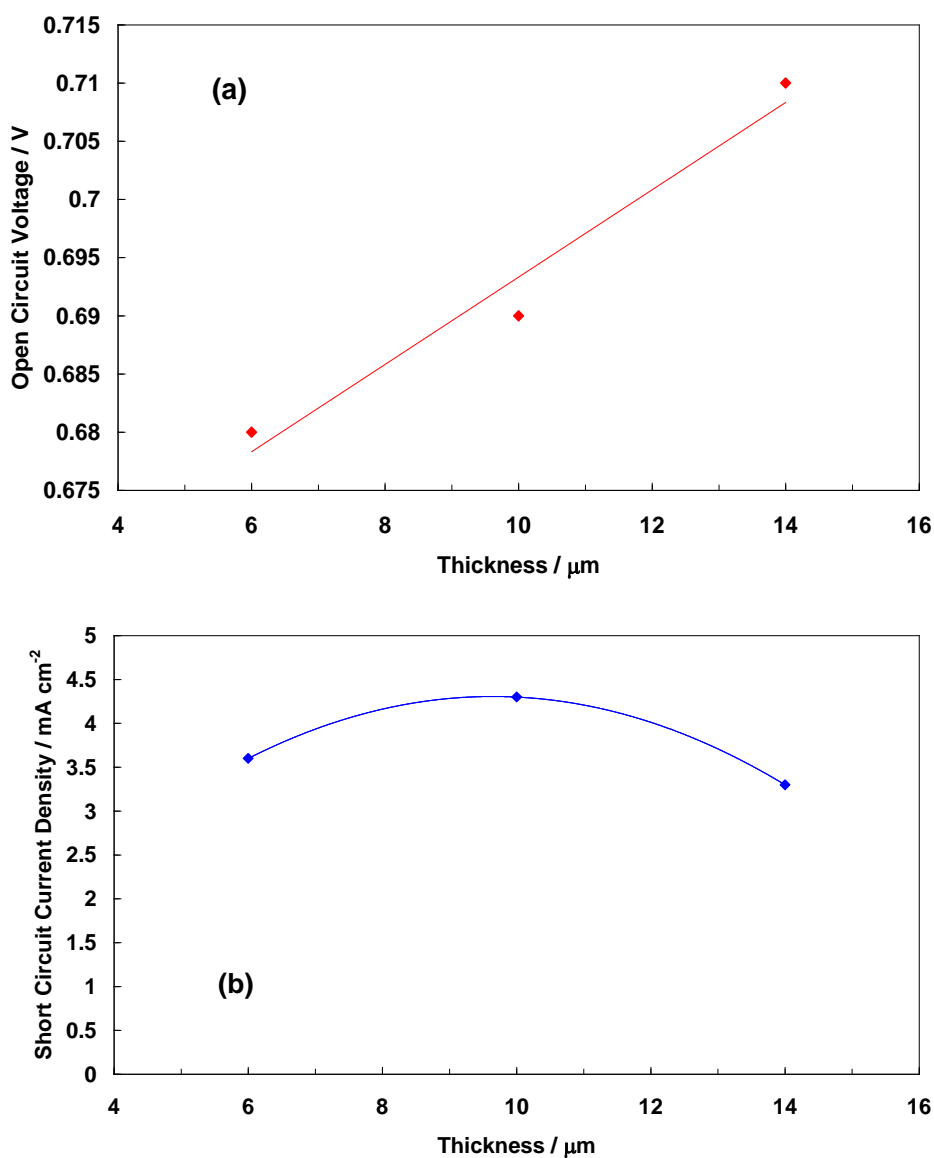
Figure 3. Variation of Open Circuit Voltage (a) and Short Circuit Current Density (b) as a function of TiO$_2$ thickness of the photo-anodes.

Fig. 3 shows the variation of V_{OC} and j_{SC} as functions of TiO_2 film thickness at the photo-anode. A linear increase of V_{OC} was recorded as the thickness of the TiO_2 films increased. This indicates that the uptake of the N3 dye in the TiO_2 layer, which acts as absorber of the incident light, increases with the thickness, as can be observed in Fig. 4; whereas, the j_{SC} showed a volcano shape behaviour with a maximum at 10 μm.
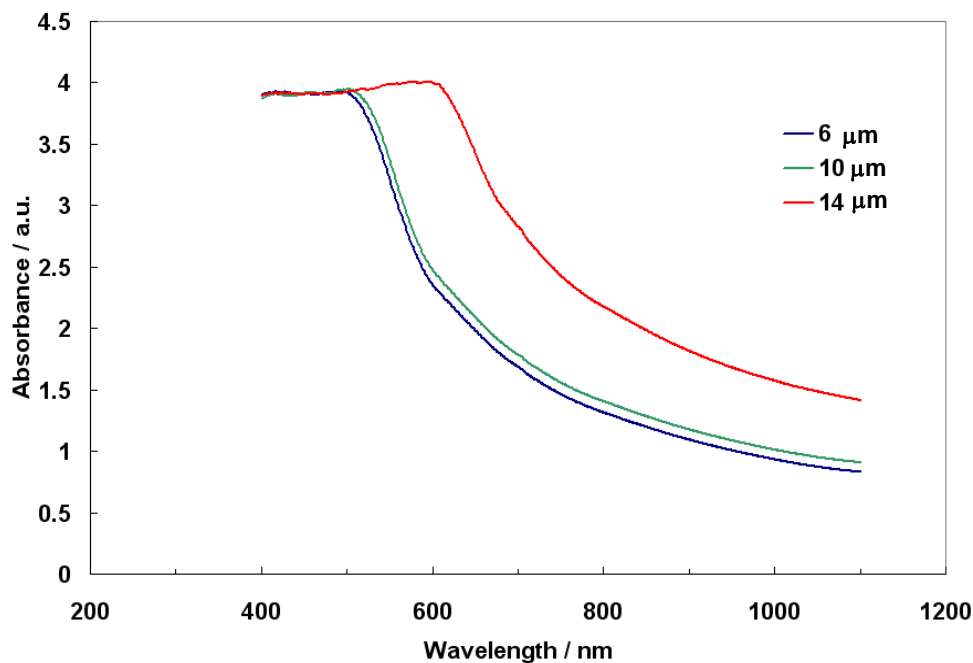
Figure 4. Absorbance spectra of the photo-anodes with different thicknesses (6, 10 and 14 μm).

This can be explained by the fact that being the diffusion lengths (Lp) similar in the three electrodes (same materials), a smaller thickness reduces the probability of recombination for the charge carrier.
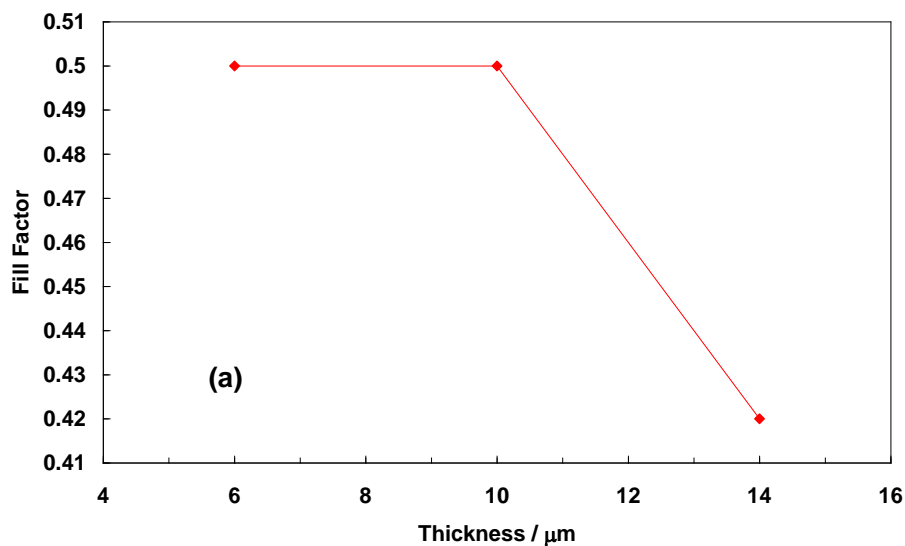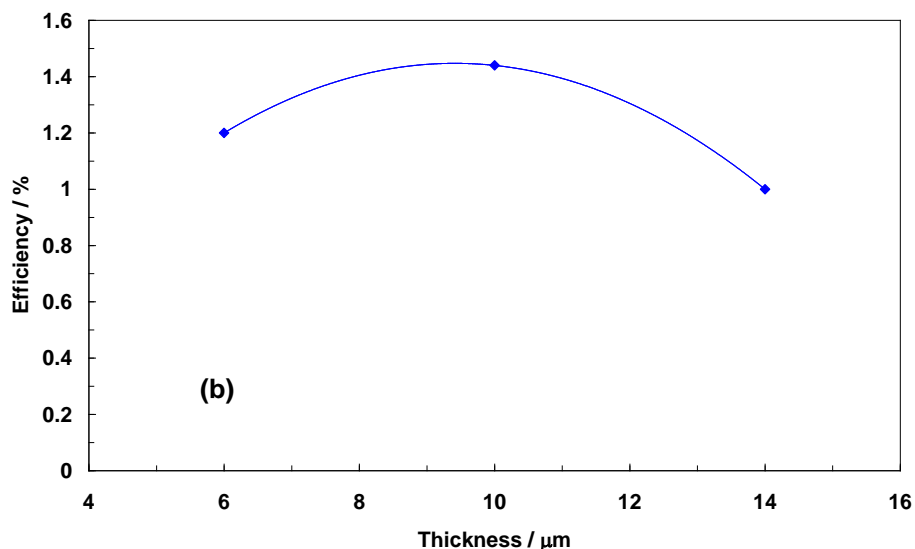
Figure 5. Variation of Fill Factor (a) and Efficiency (b) as a function of TiO_2 thickness of the photo-anodes.

Also the fill factor (see Fig. 5a) was lower for the thick electrode, indicating an increase of recombination processes caused by the high thickness of the film. On the contrary, the thinnest photo-anode is characterized by low recombination phenomena and also low capability to adsorb sun-light (Fig. 4). As a consequence of all these results, the best efficiency was achieved for the intermediate thickness of 10 μm for TiO_2 layer deposited by a spray technique (Fig. 5b).
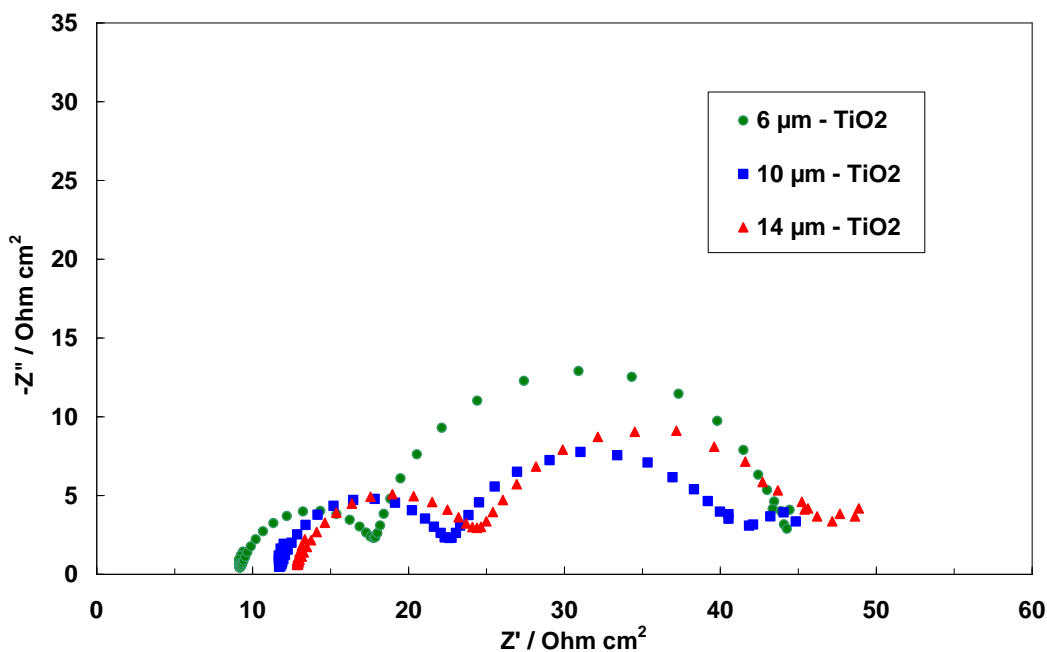
Figure 6. Electrochemical Impedance Spectra for DSSCs using TiO_2 at different thicknesses as photo-anodes.

Electrochemical Impedance Spectroscopy (EIS) has been widely used to investigate the interfacial charge transfer processes occurring in DSSCs [23]. The Nyquist plots reported in the literature for DSSCs consist of two [24] or three [23] semicircles. These are generally related, in order of decreasing frequencies, to counter-electrode/electrolyte interface, TiO_2/electrolyte interface and ionic diffusion of I_3^- species in the electrolyte. Our *ac*-impedance spectra essentially show two semicircles (Fig. 6). In addition, at very low frequencies, the onset of a linear behaviour with a slope of about 45°C is observed (Fig. 6). This is indicative of a Warburg-like diffusion component possibly related to the diffusion of ionic species at the TiO_2 interface. The *ac* response due to the diffusion of ionic species in the bulk electrolyte should occur at lower frequencies. This effect is possibly not recorded in the present spectra characterized by a low-frequency limit of 0.1 Hz (a large scattering was recorded below this frequency).

R$_{ct}$ is the charge-transfer resistance of the electrochemical reactions at the photo-anode and the counter electrode. It is observed that the counter electrode is the same in all cells, thus the R$_{ct}$ reflects the contribution for the photo-anode. The high frequency intercept measured under open circuit condition is related to the series resistance (R$_S$). It accounts for the resistance of the conductive materials in the cell with contributions from the FTO substrate layer, porous electrode material, current collector and resistivity of the electrolyte.
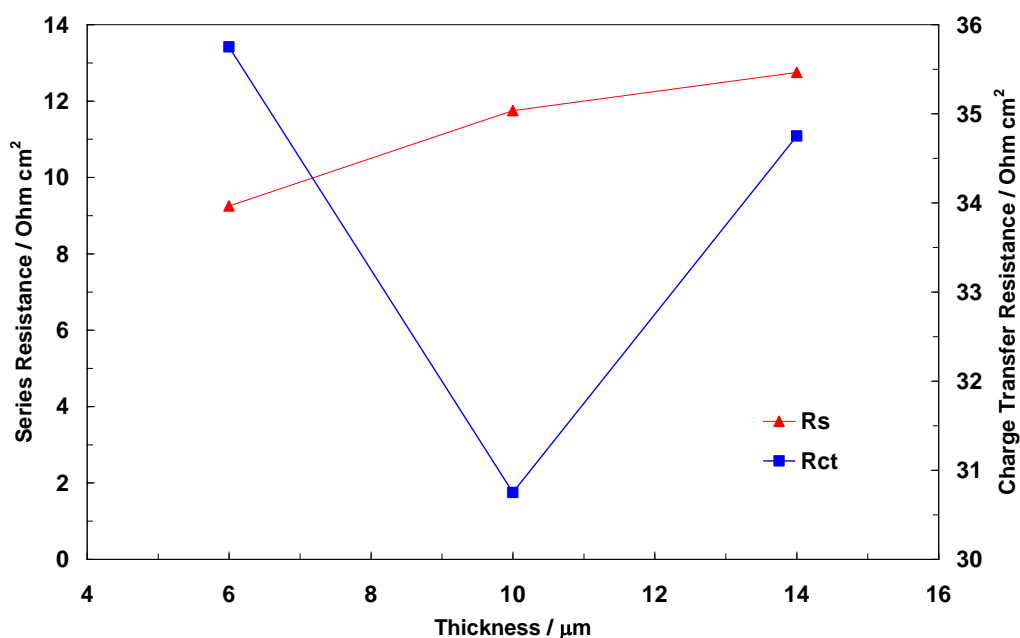
Figure 7. Variation of Series (a) and Charge Transfer (b) Resistance as a function of TiO_2 thickness of the photo-anodes.

R$_S$ and R$_{ct}$ values are reported in Fig. 7. It seems that there is not a strict correlation between R$_S$ values, which represents the ohmic contribution, and conversion efficiencies. Obviously, R$_S$ increases as the TiO_2 film thickness increases due to the fact that TiO_2 is a wide-gap semiconductor. On the contrary, conversion efficiencies appear related to reaction kinetics (R$_{ct}$). The reaction rate on the

photo-anode is strictly related to the number of oxidized dye species that are reduced by I^- ions at the interface. This trend may also indicate that beside the recombination effect and absorption characteristics, an important role is played by the amount of light (Fig. 4) that effectively reach the electrode-electrolyte interface to promote the dye transition from ground to oxidized state. Thus, it is related to the amount of dye absorbed on the TiO_2 surface and, hence, to the TiO_2 surface area and porosity. Yet, a large thickness determines a large recombination and, thus, a lower charge transfer resistance (Fig. 7). Accordingly, the photo-electrochemical performance, in terms of conversion efficiency and j_{SC}, decreased for the thick (14 μm) TiO_2 electrode (Figs. 3 and 5).

4. CONCLUSIONS

An investigation of the optimal TiO_2 film thickness at the photo-anode of a DSSC was carried out, without the use of pre- or post-layer in the photo-anode that may improve the performance, but also make more complicate the analysis of the effect played by the absorber layer. Three different thicknesses (6, 10 and 14 μm) of the TiO_2 layer were prepared by using a spray technique and a thermal treatment. Compared to the various reports in the literature, we used an easy, fast and low cost preparation procedure. A thickness of 10 μm for the TiO_2 photo-anode resulted the best compromise in terms of intensity of incident light on the N3 dye, reduction of the recombination processes, suitable series and charge transfer resistance properties. This was determined by a suitable compromise in terms of absorption of sun-light and appropriate thickness in relation to the diffusion length of photo-generated charge carriers.

References

1. M. Grätzel, *J. Photochem. Photobiol. A*, 164 (2004) 3.
2. D. Wei and G. Amaratunga, *Int. J. Electrochem. Sci.*, 2 (2007) 897.
3. L.M. Goncalves, V. de Zea Bermudez, H.A. Ribeiro and A.M. Mendes, *Energy Environ. Sci.*, 1 (2008) 655.
4. D. Soundararajan, J. K. Yoon, Y. I. Kim, J. S. Kwon, C.W. Park, S. H. Kim and J. M. Ko, *Int. J. Electrochem. Sci.*, 4 (2009) 1628.
5. H. Karami and A. Kaboli, *Int. J. Electrochem. Sci.*, 5 (2010) 706.
6. B. O'Regan and M. Grätzel, *Nature*, 353 (1991) 737.
7. A.Hagfeldt and M. Grätzel, *Acc. Chem. Res.*, 33 (2000) 269.
8. M. Grätzel, *Nature*, 414 (2001) 338.
9. M. Grätzel, *Nature*, 421 (2003) 586.
10. F.-M. Wang, C.-H. Chu, C.-H. Lee, J.-Y. Wu, K.-M. Lee, Y.-L. Tung, C.-H. Liou, Y.-Y. Wang and C.-C. Wan, *Int. J. Electrochem. Sci.*, 6 (2011) 1100.

11. L. De Marco, M. Manca, R. Giannuzzi, F. Malara, G. Melcarne, G. Ciccarella, I. Zama, R. Cingolani and G. Gigli, *J. Phys. Chem. C*, 114 (2010) 4228.
12. G. Calogero, G. Di Marco, S. Caramori, S. Cazzanti, R. Argazzi and C.A. Bignozzi, *Energy Environ. Sci.*, 2 (2009) 1162.
13. G. Rossi, G. Zanotti, N. Angelini, S. Notarantonio, A.M. Paoletti, G. Pennesi, A. Lembo, D. Colonna, A. Di Carlo, A. Reale, T.M. Brown and G. Calogero, *Int. J. Photoenergy*, (2010) art. n° 136807.
14. M. Grätzel, *J. Photochem. Photobiol. C,* 4 (2003) 145.
15. M. Grätzel, *Inorg. Chem.*, 44 (2005) 6841.
16. S. Ito, P. Chen, P. Comte, M.K. Nazeeruddin, P. Liska, P. Pechy and M. Grätzel, *Prog. Photovolt: Res. Appl.*, 15 (2007) 603.
17. S. Hore, P. Nitz, C. Vetter, C. Prahl, M. Niggemann and R. Kern, *Chem. Commun.,* 15 (2005) 2011.
18. S. Hore, C. Vetter, R. Kern, H. Smit and A. Hinsch, *Sol. Energ. Mat. Sol. Cells*, 90 (2006) 1176.
19. Z.S. Wang, H. Kawauchi, T. Kashima and H. Arakawa, *Coordinat. Chem. Rev.,* 248 (2004) 1381.
20. J.-K. Lee, B.-H. Jeong, S.-I. Jang, Y.-S. Yeo, S.-H. Park, J.-U. Kim, Y.-G. Kim, Y.-W. Jang and M.-R. Kim, *J. Mater. Sci.: Mater. Electron.,* 20 (2009) S446.
21. T. Denaro, V. Baglio, M. Girolamo, V. Antonucci, A.S. Aricò, F. Matteucci and R. Ornelas, *J. Appl. Electrochem.*, 39 (2009) 2173.
22. T. Miyasaka, M. Ikegami and Y. Kijitori, *J. Electrochem. Soc.*, 154 (2007) A455.
23. Q. Wang, J. Moser and M Grätzel, *J. Phys. Chem. B*, 109 (2005) 14945.
24. J. Van de Lagemaat, N. G. Park and A. J. Frank, *J. Phys. Chem. B*, 104 (2000) 2044.